Strong Coupling Approach to Actinide Metals

C. D. Batista,[1] J. E. Gubernatis,[1] T. Durakiewicz,[2] and J. J. Joyce[2]

[1]*Theoretical Division, Los Alamos National Laboratory, Los Alamos, New Mexico 87545, USA*

[2]*MPA Division, Los Alamos National Laboratory, Los Alamos, New Mexico 87545, USA*

(Received 18 February 2008; published 2 July 2008)

We present a strongly correlated approach to the electronic structure of actinide metals by deriving a low-energy Hamiltonian $\tilde{H}$ under the assumption that kinetic energy is small compared to Coulomb and spin-orbit interactions. The $\tilde{H}^{\mathrm{Pu}}$ for Pu metal is similar to the models used for Ce and other lanthanides but qualitatively different from the $\tilde{H}$ presented for the rest of the actinides. With $\tilde{H}^{\mathrm{Pu}}$, we computed the photoemission spectrum and specific heat for α and δ-Pu and found good agreement with experiment.

DOI: 10.1103/PhysRevLett.101.016403 PACS numbers: 71.10.−w, 71.27.+a, 75.30.Mb

Introduction.—Modeling the actinides and their compounds is challenging because they are generally strongly correlated materials. Because electronic structure methods, such as the local density approximation (LDA), often fail to capture what is observed experimentally at low energies, theoretical studies of strongly correlated $3d$ and $4f$ materials have traditionally relied on many-body models to capture such physical phenomena as itinerant ferromagnetism, antiferromagnetism, heavy fermion, and non-Fermi liquid behavior, as well as unconventional superconductivity. A similar spectrum of behavior is observed in $5f$ electron materials; however, novel modeling is needed because of the multiple competing interactions that appear in their energy scale hierarchy.

We recall that for $3d$ electron materials, multiorbital Hubbard models are commonly evoked, while the periodic Anderson model (PAM) is standard for describing $4f$-materials. Both models treat the Coulomb interaction by an on-site contribution that penalizes the double electron occupancy of local atomic orbitals contributing to the valence band. Kinetic energy is modeled by orbital overlap. For lanthanide systems, the $f-f$ overlap is usually neglected due to the strong localization of the $4f$-orbitals.

Similar modeling for actinide materials requires some different features. One important difference relative to lanthanide materials is the relevance of the $f-f$ overlap due to the larger extension of the $5f$-orbitals. In the model to be presented, we let the local electronic structure vary from site to site, but the local valences are restricted to be f^n or f^{n+1} due to our assumption of on-site Coulomb and spin-orbit interactions much larger than kinetic energy terms. Under this assumption, we derive the lowest-energy multiplet of each configuration (f^n or f^{n+1}) and treat the kinetic energy as a perturbation. The resulting Hamiltonian differs from the one in [1–3] by including $f-d$ hybridization. It is important to note that the lowest-energy multiplet of each configuration can be derived for any intermediate coupling scheme between LS and $j-j$. The form of the low-energy Hamiltonian remains the same because the total angular momentum of the multiplet does not change with the coupling scheme.

Below, we will sketch the derivation of the model, present calculations of the photo-emission spectrum (PES), and compare these predictions with the measured spectra for α and δ-Pu. Like the LDA + DMFT treatment of [4], our simpler model reproduces the low-energy contributions to the PES. We will also compute the specific heat coefficients γ_α and γ_δ. However, our most striking finding will be the cancellation of the $f-f$ hopping at low energies and the consequent similarity between Pu and Ce or mixed valent Sm at low energies.

Model.—We start by considering a multiband model for $5f$-electrons which includes intra-atomic and interatomic (hopping) terms for the f-orbitals, plus $d-f$ hybridization: $H = H_d + H_{df} + H_f$, where

$$\begin{aligned} H_d &= \sum_{\mathbf{k},l,\sigma\mathbf{z}} \epsilon_{\mathbf{k},l_z} d^\dagger_{\mathbf{k}l_z\sigma} d_{\mathbf{k}l_z\sigma} \\ H_{df} &= \sum_{\mathbf{k},l,\sigma\mathbf{z}} V_{\mathbf{k},l_z} d^\dagger_{\mathbf{k}l_z\sigma} f_{\mathbf{k}l_z\sigma} + V^*_{\mathbf{k},l_z} f^\dagger_{\mathbf{k}l_z\sigma} d_{\mathbf{k}l_z\sigma} \\ H_f &= H_{\mathrm{Coul}} + H_{\mathrm{SO}} + H_{\mathrm{K}} + H_{\mathrm{CEF}} \end{aligned} \tag{1}$$

with

$$\begin{aligned} H_{\mathrm{SO}} &= \lambda \sum_{\mathbf{i},l_z,l'_z,\sigma,\sigma'} \zeta_{l_z\sigma,l'_z\sigma'} f^\dagger_{\mathbf{i}l_z\sigma} f_{\mathbf{i}l'_z\sigma'} \\ H_{\mathrm{K}} &= \sum_{\mathbf{i},\mathbf{r},l_z,l'_z,\sigma} t^{\mathbf{r}}_{l_z,l'_z} (f^\dagger_{\mathbf{i}l_z\sigma} f_{\mathbf{i}+\mathbf{r}l'_z\sigma} + f^\dagger_{\mathbf{i}+\mathbf{r}l'_z\sigma} f_{\mathbf{r}l_z\sigma}) \\ H_{\mathrm{CEF}} &= \sum_{\mathbf{i},l_z,l'_z,\sigma} (\epsilon_f \delta_{l_z,l'_z} + B_{l_z,l'_z}) f^\dagger_{\mathbf{i}l_z\sigma} f_{\mathbf{i}l'_z\sigma}. \end{aligned} \tag{2}$$

The operators $f^\dagger_{\mathbf{k}l_z\sigma} = \frac{1}{\sqrt{N}} \sum_{\mathbf{r}} e^{i\mathbf{k}\cdot\mathbf{r}} f_{\mathbf{r}l_z\sigma}$ and $d^\dagger_{\mathbf{k}l_z\sigma} = \frac{1}{\sqrt{N}} \sum_{\mathbf{r}} e^{i\mathbf{k}\cdot\mathbf{r}} d_{\mathbf{r}l_z\sigma}$ create f and d electrons in momentum space with angular momentum l and projection l_z (N is the number of lattice sites). H_d describes a broad d-band (it can also have s or p-character) that is hybridized with the f-orbitals via H_{df}. In H_f, H_{Coul} (not displayed) contains all the intra- and interorbital on-site f-f Coulomb interactions. λ is the spin-orbit coupling, and the matrix elements $\zeta_{l_z\sigma,l'_z\sigma'}$ are: $\zeta_{l_z\sigma,l_z\sigma} = l_z\sigma/2$, $\zeta_{l_z+1\downarrow,l_z\uparrow} = \sqrt{12 - l_z(l_z+1)}/2$, $\zeta_{l_z-1\uparrow,l_z\downarrow} = \sqrt{12 - l_z(l_z-1)}/2$, and zero for other cases.

$H_{\rm K}$ describes the f-electron kinetic energy due to orbital overlap with $t^{\mathbf{r}}_{l_z,l'_z}$ being the hopping integrals between the l_z and l'_z orbitals of two ions separated by a relative vector $\mathbf{r}$. In $H_{\rm CEF}$, B_{l_z,l'_z} is the Hermitian crystal field matrix [3], and ϵ_f is the average energy of the f-orbitals.

Effective model.—We now consider the strong coupling limit of H when the intra-atomic interactions $H_{\rm Coul}$ and $H_{\rm SO}$ are much bigger than the f-f hopping and hybridization terms in $H_{\rm K}$ and H_{df}. In this limit, we need to diagonalize the intra-atomic terms ($H_{\rm Coul} + H_{\rm SO}$) and treat $H_{\rm K}$ and H_{df} as perturbations. The first consequence of this approach is that no more than two different $5f$ valences, $5f^n$ and $5f^{n+1}$, can appear in the low-energy spectrum, $E \ll U$, where U is the characteristic magnitude of $H_{\rm Coul}$. States containing other $5f$ configurations have energies of order U higher than the low-energy states. The lowest-energy multiplet of $H_{\rm Coul} + H_{\rm SO}$ has total angular momentum $|L - S|$ (for $n + 1 < 7$), where S is the maximum total spin of the configuration and L is the maximum orbital angular momentum for that value of S. Either n or $n + 1$ is an odd number. We will use J (I) for the total angular momentum of the f-configuration that has an odd (even) number of electrons. Therefore, if there are M sites in the even configuration and $N - M$ sites in the odd configuration, the lowest-energy subspace $\mathcal{S}$ of $H_{\rm Coul} + H_{\rm SO}$ consists of $\binom{N}{M}$ different charge configurations, each of which has a $(2I + 1)^M(2J + 1)^{N-M}$ different states due to the angular momentum degree of freedom.

We use a hard-core boson operator $a_{\mathbf{i}I_z}$ ($a^\dagger_{\mathbf{i}I_z} a^\dagger_{\mathbf{i}I'_z} = 0$) to represent the lowest-energy multiplet of the even configuration and a constrained fermion operator $c_{\mathbf{i}J_z}$ ($c^\dagger_{\mathbf{i}J_z} c^\dagger_{\mathbf{i}J'_z} = 0$) to represent the lowest-energy multiplet of the odd configuration. To first order in the perturbation, the low-energy effective Hamiltonian $\tilde{H}$ results from projecting $H_{\rm K} + H_{fd}$ into $\mathcal{S}$:

$$\begin{aligned}
\tilde{H} &= \tilde{H}_d + \tilde{H}_{df} + \tilde{H}_f \\
\tilde{H}_d &= \sum_{\mathbf{k},I_z,J_z} \tilde{\epsilon}_{\mathbf{k},|J_z-I_z|} \tilde{d}^\dagger_{\mathbf{k}J_z-I_z} \tilde{d}_{\mathbf{k}J_z-I_z} \\
\tilde{H}_{df} &= \sum_{\mathbf{k},\mathbf{q},I_z,J_z} (\tilde{V}_{\mathbf{k},J_z-I_z} \tilde{d}^\dagger_{\mathbf{k}J_z-I_z} a^\dagger_{\mathbf{q}I_z} c_{\mathbf{k}+\mathbf{q}J_z} + \text{H.c.}) \\
\tilde{H}_f &= \sum_{\mathbf{i},\mathbf{r},I_z,J_z,I'_z,J'_z} \tau^{\mathbf{r}}_{J_zI_z,J'_zI'_z} (c^\dagger_{\mathbf{i}J'_z} c_{\mathbf{i}+\mathbf{r}J_z} a^\dagger_{\mathbf{i}+\mathbf{r}I'_z} a_{\mathbf{i}I_z} + \text{H.c.}) \\
&\quad + \sum_{\mathbf{i},I_z,I'_z} A_{I_z,I'_z} a^\dagger_{\mathbf{i}I'_z} a_{\mathbf{i}I_z} + \sum_{\mathbf{i},J_z,J'_z} C_{J_z,J'_z} c^\dagger_{\mathbf{i}J'_z} c_{\mathbf{i}J_z}.
\end{aligned} \tag{3}$$

The matrix elements of $\tau^{\mathbf{r}}$, A, and C are

$$\tau^{\mathbf{r}}_{J_zI_z,J'_zI'_z} = \langle \mathbf{i}, J'_z | \langle \mathbf{i}+\mathbf{r}, I'_z | H_{\rm K} | \mathbf{i}, I_z \rangle | \mathbf{i}+\mathbf{r}, J_z \rangle, \tag{4}$$

$$A_{I_z,I'_z} = \langle \mathbf{i}, I'_z | H_{\rm CEF} | \mathbf{i}, I_z \rangle, \tag{5}$$

$$C_{J_z,J'_z} = \langle \mathbf{i}, J'_z | H_{\rm CEF} | \mathbf{i}, J_z \rangle, \tag{6}$$

where $|\mathbf{i}, J_z\rangle$ ($|\mathbf{i}, I_z\rangle$) denotes the state of the site $\mathbf{i}$ with total angular momentum J (I) and projection J_z (I_z). These single atom states are computed using the coupling scheme (LS, $j-j$ or intermediate) that is adequate for each actinide [5]. The terms of $\tilde{H}_f$ correspond to the exchange of the $5f^n$ and $5f^{n+1}$ configurations on sites $\mathbf{i}$ and $\mathbf{i} + \mathbf{r}$. This exchange occurs when an electron hops from the site in the $5f^{n+1}$ configuration to the site that was in the $5f^n$ state. $\tilde{H}_{fd}$ is a hybridization term for the effective quasiparticles with $\tilde{d}$ orbitals that have angular momentum $J_z - I_z$ and a dispersion relation $\tilde{\epsilon}_{\mathbf{k},|J_z-I_z|}$. We leave $\tilde{\epsilon}_{\mathbf{k},|J_z-I_z|}$ and $\tilde{V}_{\mathbf{k},J_z-I_z}$ as free parameters.

Case of Pu.—The effective Hamiltonian $\tilde{H}$ describes the general situation of valence fluctuations between two magnetic configurations. For metallic Pu, they are $5f^5(J = 5/2)$ and $5f^6(I = 0)$, which makes Pu one of simplest cases to treat because the bosonic $5f^6$ configuration is nonmagnetic. Therefore, the corresponding effective boson can be replaced by an empty site, and $c^\dagger_{\mathbf{i}J_z}$ creates a hole with angular momentum J and projection J_z. This replacement leads to a simpler form of $\tilde{H}^{\rm Pu}$:

$$\begin{aligned}
\tilde{H}^{\rm Pu} &= \sum_{\mathbf{i},\mathbf{r},J_z,J'_z} \tau^{\mathbf{r}}_{J_z,J'_z} (c^\dagger_{\mathbf{i}J'_z} c_{\mathbf{i}+\mathbf{r}J_z} + \text{H.c.}) + \sum_{\mathbf{i},J_z,J'_z} C_{J_z,J'_z} c^\dagger_{\mathbf{i}J'_z} c_{\mathbf{i}J_z} \\
&\quad + \sum_{\mathbf{k},J_z} \tilde{\epsilon}_{\mathbf{k},J_z} \tilde{d}^\dagger_{\mathbf{k}J_z} \tilde{d}_{\mathbf{k}J_z} + (\tilde{V}_{\mathbf{k},J_z} \tilde{d}^\dagger_{\mathbf{k}J_z} c_{\mathbf{k}J_z} + \text{H.c.}),
\end{aligned} \tag{7}$$

which is an extended version of the infinite U Periodic Anderson model (PAM) since it includes the $f - f$ hopping term that is significant for $5f$ systems. The angular momentum of each fermion is J, and the hopping amplitude $\tau^{\mathbf{r}}_{J_z,J'_z}$ depends on the initial and final values of J_z and on the bond orientation. These dependencies are direct consequences of the strong spin-orbit interaction (2).

Self-evident from the form of $\tilde{H}^{\rm Pu}$ is the existence of only one *effective fermion* propagating across the lattice despite there being 5 and 6 electrons in each of the stable valence configurations of Pu. This simplification is a natural consequence of the strong Coulomb intra-atomic interactions [2] and the reason why a "dual" $5f$-electron behavior (some of the $5f$-electrons being partially localized) has to be enforced in band structure calculations [6] to reproduce the properties of Pu.

Far from being evident is the observation that the hopping tensor $\tau^{\mathbf{r}}_{J_z,J'_z}$ vanishes for the particular case of Pu. This surprising result is a consequence of the particular valence of Pu and the ratios between the different single-particle hopping amplitudes, $t^{\mathbf{r}}_{l_z,l'_z} = \delta_{l_z,l'_z} t^{\mathbf{r}}_{l_z}$,

$$t^{\mathbf{r}}_0 = 20t^{\mathbf{r}}, \qquad t^{\mathbf{r}}_1 = -15t^{\mathbf{r}}, \qquad t^{\mathbf{r}}_2 = 6t^{\mathbf{r}}, \qquad t^{\mathbf{r}}_3 = -t^{\mathbf{r}}, \tag{8}$$

as computed by Harrison and Wills [7]. (Time reversal symmetry requires $t^{\mathbf{r}}_{l_z} = t^{\mathbf{r}}_{-l_z}$.) $t^{\mathbf{r}}_{l_z,l'_z}$ is diagonal because we are choosing the quantization axis parallel to $\mathbf{r}$ and assuming invariance under rotations along $\mathbf{r}$ (i.e., $t^{\mathbf{r}}_{l_z,l'_z}$ is the hopping tensor of the isolated bond $[\mathbf{i}, \mathbf{i} + \mathbf{r}]$).

The cancellation of $\tau^{\mathbf{r}}_{J_z,J'_z}$ is independent of the amplitude $t^{\mathbf{r}}$ and of the crystal structure (it is a property of the bond between two sites). Briefly, it occurs because there are two single-particle hopping processes in $H_{\rm K}$ that contribute to

$\tau^{\mathbf{r}}_{J_z,J_z}$: an electron hops from the $5f^6$ configuration at site $\mathbf{i}$ to the $5f^5$ configuration at site $\mathbf{i}+\mathbf{r}$ with either $l_z = J_z + 1/2$ and $S_z = -1/2$ or $l_z = J_z - 1/2$ and $S_z = 1/2$. From (8), $t_{J_z+1/2}$ and $t_{J_z-1/2}$ have opposite signs so destructive interference occurs. Pu is the only case for which they also have the same magnitude [8], thus producing a blocking of the effective $f-f$ hopping for the lowest-energy $J = 5/2$ multiplet. ($\tau^{\mathbf{r}}_{J_z,J'_z}$ is nonzero for the first excited $J = 7/2$ multiplet.) This blocking implies that the low-energy theory for Pu is the usual PAM used to describe $4f$-elements like Ce ($4f^1$) that also contains a low-energy $5/2$ multiplet and an excited $J = 7/2$ multiplet. A detailed proof of this blocking will be given elsewhere [8].

Photoemission.—We will now consider the angle-integrated photoemission spectrum (PES) that results from the effective model $\tilde{H}^{\mathrm{Pu}}$. In the "sudden approximation," the $T = 0$ spectral density $A(\omega)$ is given by

$$A(\omega) = \sum_{l_z,\sigma,n} |\langle \phi_n | \hat{f}_{\mathbf{i}l_z\sigma} | \psi_0 \rangle|^2 \delta(\omega - E_n + E_0) \qquad (9)$$

where $|\psi_0\rangle$ is the ground state of H in the N_p-particle subspace while $|\phi_n\rangle$ are the eigenstates of H in the $N_p - 1$ particle subspace. The incident photon emits an electron from a given site leading to a transition to a final state $|\phi_n\rangle$ whose relative energy equals the difference between the initial and the final photon energies. According to Fermi's golden rule, the probability of such a transition is given by $|\langle \phi_n | \hat{f}_{l_z\sigma} | \psi_0 \rangle|^2$. The electron can be emitted either from an atom in the $5f^5$ or $5f^6$ configuration. The first transition leads to final $5f^4$ configuration whose energy is too high in the large U limit. Therefore, because the final atomic state is a $5f^5$ configuration, only the second transition contributes to the "low-energy spectrum" ($|\omega| \ll U$). To compute the low-energy PES with $\tilde{H}^{\mathrm{Pu}}$, we have to project $\hat{f}_{l_z\sigma}$ into $\mathcal{S}$. Then,

$$\tilde{A}(\omega) = \alpha_{5/2} \sum_{J_z=-5/2,n}^{5/2} |\langle \tilde{\phi}_n | c^\dagger_{\mathbf{i}5/2J_z} | \tilde{\psi}_0 \rangle|^2 \delta(\omega - E_{n0}) + \alpha_{7/2} \sum_{J_z=-7/2,n}^{7/2} |\langle \tilde{\phi}_n | c^\dagger_{\mathbf{i}7/2J_z} | \tilde{\psi}_0 \rangle|^2 \delta(\omega - E_{n0}), \qquad (10)$$

with $E_{n0} = E_n - E_0$. Here, we are keeping not only the lowest-energy $J = 5/2$ multiplet described by $c^\dagger_{\mathbf{i}5/2J_z}$, but also the excited $J = 7/2$ multiplet described by the $c^\dagger_{\mathbf{i}7/2J_z}$ fermion operator. This is necessary if we want the PES spectrum over a range of $\sim$1 eV away from the Fermi level. To understand the origin of (10), we first note that the electron emitted from the nonmagnetic $5f^6$ configuration can have total angular momentum $J = 5/2$ or $J = 7/2$ ($l = 3$ and $S = 1/2$). In the low-energy subspace $\mathcal{S}$, this corresponds to the creation of an effective hole ($5f^5$ configuration) with $J = 5/2$ or $J = 7/2$. The coefficients

$$\alpha_J = \sum_{l_z,\sigma} |\langle \mathbf{i}, J, J_z | \hat{f}_{l_z\sigma} | \mathbf{i}, I = 0 \rangle|^2,$$

are the probabilities of the final state belonging to the low-energy subspace with total angular momentum $J = 5/2$ or $7/2$. By using a simple LS coupling scheme, we obtain $\alpha_{5/2} \simeq 0.15$ and $\alpha_{7/2} \simeq 0.28$. The ratio $\alpha_{5/2}/\alpha_{7/2}$ will be smaller for a more realistic intermediate coupling scheme [5], but that level of accuracy is not required here given the lack of high-resolution resonant PES data. The $J = 7/2$ multiplet has a diagonal spin-orbit energy $\simeq 0.75$ eV relative to the $J = 5/2$ multiplet [see (2)]. Since $c^\dagger_{\mathbf{i}JJ_z}$ creates a hole in the closed shell $5f^6$ configuration, the low-energy PES of H is obtained from the *inverse* PES spectrum of $\tilde{H}^{\mathrm{Pu}}$ [compare Eqs. (9) and (10)].

Because of the lack of controllable approaches for solving the PAM, we will assume that the intersite correlations between f-states are weak within the energy scale of the PES experiment and use the single-impurity approximation. Specifically, we used the variational method introduced by Gunnarsson and Schönhammer [9] where we assumed a uniform density of states for the d-band and a bandwidth of $2D$ with $D = 5$ eV. To minimize the number of free parameters, we set the crystal field term to zero and assumed $\tilde{V}_{\mathbf{k}JJ_z} = V$. V and D determine the effective hybridization parameter $\Delta = \pi V^2/D$. We define $\tilde{\epsilon}_f$ as the energy of the (unhybridized) $5f^5$ ($J = 5/2$) configuration relative to the Fermi level. We used $\tilde{\epsilon}_f = -2$ eV and $\Delta = 0.15$ eV for δ-Pu and $\Delta = 0.2$ eV for α-Pu.

Angle-integrated PES measurements were performed on polycrystalline samples of α-Pu and δ-Pu. We used a tunable Laser Plasma Light Source to measure the resonant PES with incident photon energy $h\nu = 115$ eV, and a He lamp with $h\nu = 40.8$ eV to obtain higher energy resolution. The resonant PES spectrum is only available for δ-Pu. The instrumental resolution was 60 meV for $h\nu = 40.8$ eV and 150 meV at resonance [10]. For $h\nu = 40.8$ eV, the photo-ionization cross sections for Pu-$6d$ and Pu-$5f$ orbitals are similar while for $h\nu = 115$ eV, the Pu $5f$-character dominates the spectral density [11].

To compare with our theory for the low-energy spectrum, we performed a data analysis that separates the low and high-energy contributions. We fitted $h\nu = 40.8$ eV experimental data for α-Pu and δ-Pu by a nonlinear regression method using a convolution of three peaks, the Fermi function, and the background. Each peak contained a Lorentzian and a Gaussian component as well as intrinsic asymmetry. The calculated density of states was convoluted with the Fermi function for $T = 77$ K and an experimental resolution of 60 meV. The experimental data, fittings, and theoretical predictions are plotted in Fig. 1. All spectra were normalized to maximum intensity.

Figures 1(a) and 1(b) also show the comparison between the fits and the calculation based on $\tilde{H}^{\mathrm{Pu}}$. The peak closest to E_F corresponds to transitions from the nonmagnetic $5f^6$ state to the $J = 5/2$ $5f^5$ lowest-energy multiplet. The second peak comes from the transitions to the first excited

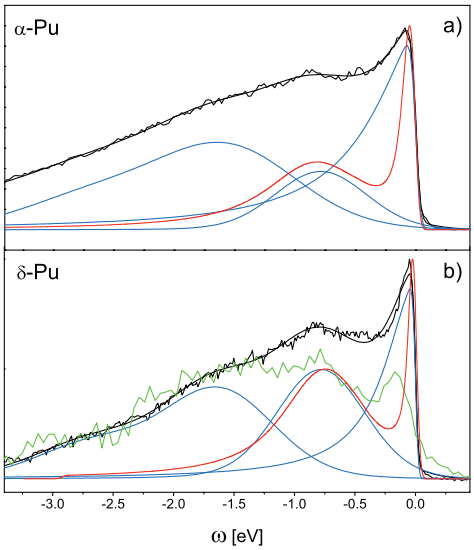

FIG. 1 (color). Measured angle-integrated PES for α-Pu (a) and δ-Pu (b). Experimental data and fit (explained in the text) are shown in black lines. The different peak components obtained from the fit are shown as blue lines, while the result of (10), convoluted with the experimental conditions (see text), is shown in red. Panel (b) also shows the $h\nu = 115$ eV Fano resonance scan for δ-Pu as a green line.

$J = 7/2$ multiplet. The splitting between these two peaks is mainly determined by the spin-orbit coupling. The $J = 7/2$ peak has an intrinsic additional broadening due to the finite value of $\tau^{\mathbf{r}}_{J_z,J'_z}$ for this multiplet. This broadening is of the order of the single $J = 7/2$ bandwidth $W \simeq 0.35$ eV. We incorporated it into the $J = 7/2$ peak. Our low-energy effective model does not reproduce the spectral weight that appears at energies $\gtrsim 1.5$ eV because this contribution comes from the high-energy states that were projected out in the derivation of $\tilde{H}^{\mathrm{Pu}}$. Since only the nonmagnetic ($J = 0$) $5f^6$ configuration appears at low energies, these states must correspond to the $J = 5/2$ and $J = 7/2$ multiplets of the $5f^5$ configuration that have higher energy because they do not obey the Hund's rules (like ^6P and ^6F states) and $5f^4$ final states at even higher energies. Although the energy scales are different, similar low- and high-energy contributions to the PES have been measured for SmS [12] that is a $4f$ analog of Pu because the Sm ion fluctuates between Sm^{2+} ($4f^6$) and Sm^{3+} ($4f^5$).

Our calculation also misses some spectral weight between the two peaks because only the $5f$ contribution is included, while the measured PES contains contributions from the broad d-band. This contribution is reduced when the energy of the incident photons is in resonance with the $5f$-component ($h\nu = 115$ eV). The main difference between the measured spectra for $h\nu = 40.8$ eV ($5f$-resonance) and $h\nu = 115$ eV appears between the two peaks [Fig. 1(b)]. Thus, a significant amount of the measured spectral weight between the two peaks (for $h\nu = 40.8$ eV) comes from off-resonance effects that are beyond the scope of our calculation [13].

The parameters obtained from fitting the PES spectra lead to the following values of the specific heat coefficients: $\gamma_\delta = 44$ mJ/mol K^2 in good agreement with the measured value of 42.3 mJ/mol K^2 reported in [14] and 33–55 mJ/mol K^2 reported in [15]. Our $\gamma_\alpha = 9$ mJ/mol K^2 is smaller than the value of 17 mJ/mol K^2 reported in [16]. These parameters also place α and δ-Pu in a mixed valence regime with f-occupancies: $\langle n_f \rangle = 5.14$ for δ-Pu and $\langle n_f \rangle = 5.25$ for α-Pu ($n_f = \sum_{l_z,\sigma} f^\dagger_{\mathbf{i}l_z\sigma} f_{\mathbf{i}l_z\sigma}$).

Discussion.—The cancellation of the $f - f$ hopping tensor at low energies is a unique characteristic of the Pu metal that makes its low-energy model qualitatively similar to the one used for Ce or mixed valent Sm [12]. This similarity could be the common root for explaining the huge volume expansions observed in both elements. There are several implications of immediate relevance: Magnetism is strongly suppressed in $\tilde{H}^{\mathrm{Pu}}$ when the concentration of f-electrons differs significantly from an integer value, and our results place both α and δ-Pu in the mixed valence regime in agreement with the observed lack of magnetic ordering [14,17]. In contrast, a serious limitation of band structure calculations is that the *ad hoc* hypothesis of partial localization leads to magnetic ordering in δ-Pu [18].

We thank E. Bauer, J. Thompson, and J. Lawrence for useful discussions. We acknowledge support by the DOE LDRD program, Office of Science, and Campaign 2.

[1] G. Zwicknagl, A. N. Yaresko, and P. Fulde, Phys. Rev. B **65**, 081103(R) (2002).
[2] D. V. Efremov *et al.*, Phys. Rev. B **69**, 115114 (2004).
[3] T. Hotta, Rep. Prog. Phys. **69**, 2061 (2006).
[4] J. H. Shim, K. Haule, and G. Kotliar, Nature (London) **446**, 513 (2007); J.-X. Zhu *et al.*, Phys. Rev. B **76**, 245118 (2007).
[5] G. van der Laan *et al.*, Phys. Rev. Lett. **93**, 097401 (2004); K. T. Moore *et al.*, Phys. Rev. B **76**, 073105 (2007).
[6] J. M. Wills *et al.*, J. Electron Spectrosc. Relat. Phenom. **135**, 163 (2004).
[7] W. A. Harrison, Phys. Rev. B **28**, 550 (1983); J. M. Wills and W. A. Harrison, Phys. Rev. B **28**, 4363 (1983).
[8] C. D. Batista (to be published).
[9] O. Gunnarsson and K. Schönhammer, Phys. Rev. Lett. **50**, 604 (1983); Phys. Rev. B **28**, 4315 (1983).
[10] A. J. Arko *et al.*, Phys. Rev. B **62**, 1773 (2000); E. D. Bauer *et al.*, Mater. Res. Soc. Symp. Proc. **893**, 125 (2006).
[11] J. J. Yeh and I. Lindau, At. Data Nucl. Data Tables **32**, 1 (1985).
[12] A. Chainani *et al.*, Phys. Rev. B **65**, 155201 (2002).
[13] O. Gunnarson and T. C. Li, Phys. Rev. B **36**, 9488 (1987); C. Laubschat *et al.*, Phys. Scr. **41**, 124 (1990).
[14] J. C. Lashley *et al.*, Phys. Rev. B **72**, 054416 (2005).
[15] P. Javorsky *et al.*, Phys. Rev. Lett. **96**, 156404 (2006).
[16] J. C. Lashley *et al.*, Phys. Rev. Lett. **91**, 205901 (2003).
[17] R. H. Heffner *et al.*, Phys. Rev. B **73**, 094453 (2006).
[18] P. Söderlind and B. Sadigh, Phys. Rev. Lett. **92**, 185702 (2004).